The dynamics and event-collision bifurcations in switched control systems with delayed switching

Piotr Kowalczyk*

July 8, 2019

Abstract

We analyse a switched control system with negative feedback and delayed switching. In particular, we consider the effects of small and arbitrary delays in the switching decision function on the asymptotic dynamics of the system. In the absence of time delay, the phase space contains a set of points which under the action of the system flow are bounded, and trajectories rooted at these points converge to neutrally stable pseudo-equilibria in finite time. This structure is destroyed under the introduction of time delay. For a sufficiently small time delay, the bounded trajectories converge to a unique small scale limit cycle attractor. This is shown by means of the so-called delayed switching lines. For larger delay times, we observe event-collision bifurcations, symmetry breaking bifurcations, homoclinic bifurcations and multistability. For larger time delays, the delayed switching lines play an important role as they may be used to determine the stability properties of limit cycle attractors. By means of the discontinuity mapping, we show why following an event-collision bifurcation the stability of a limit cycle attractor may be radically altered. Our numerical test-bed model we consider here may be used on the macroscopic scale as a model for human neuromuscular control during quiet standing or target tracking. It is interesting that much of the complex dynamics we uncover here occurs in the parameter range of delay time of around 150ms, which is a typical processing time of neurocontrol systems of healthy human subjects during the control of, for example, quiet standing.

Keywords: Event-collision bifurcations, limit cycles, switched control systems

1 Introduction

In recent decades much of research effort has been devoted to investigate the dynamics of systems which are piecewise-smooth, e.g. [9, 14, 1, 13, 5, 6] among many other works. This interest has been sparked by a wide range of applicability of such systems to model, especially on the macroscopic scale, systems of

*Department of Mathematics, Building C-11, room 4.10, Wrocław University of Science and Technology, Janiszewskiego 14a, 50-372 Wrocław, Poland, Email: piotr.s.kowalczyk@pwr.edu.pl

relevance to applications in control and mechanical engineering, as well as in biomechanics [15, 16] or neuroscience [4].

A piecewise-smooth system typically losses its smoothness properties on a manifold, so-called switching manifold, which can be defined as a zero level set of some function, which we term a switching function. This function acts like a switch between differentiable vector fields. A special class of piecewise-smooth systems are systems which are characterised by the presence of time delay in the function which determines the switching [18, 19, 20, 11]. Such systems naturally arise in switched control strategies where there is a deliberate time lag between the instance when a switching manifold is crossed, and the time when the actual switch takes place. This is the so-called "act-and-wait" control strategy [10]. A simple example of such a strategy would be a two-step control of a one-degree-of-freedom inverted pendulum. Let us suppose that we wish to keep an inverted pendulum, which is being continuously perturbed, in an upright position. It turns out that the best strategy to keep the inverted pendulum bounded in a region around its unstable upside-down equilibrium is by gently tapping the pendulum when it is off the vertical position by some angle, and thus bring it back to the neighbourhood of the unstable upside-down equilibrium. The switched control is not applied instantaneously, after the unstable vertical position is crossed, but it is applied after certain delay time. Introducing delay time implies that the phase space of the system is no longer finite dimensional and to fully describe the dynamics a history segment of a trajectory is required. However, due to the fact that the delay time is present only in the switching function, and not in the state variable, the investigations of system dynamics may be reduced to studies of finite dimensional maps, as it was shown, for example, in [18].

In the paper, we consider a planar switched control model with negative feedback and time delay in the switching function. Strictly speaking, as discussed above, the phase space of the model system is infinite dimensional due to the presence of time delay. The proposed model system is a variation of an act-and-wait macroscopic model of, for examples, target tracking or neuromuscular human balance control during quiet standing [2, 3, 12]. In particular, to simplify the model system, we assume that the control torque is constant over some time required to change the position and velocity so that the inverted pendulum may be brought back inside some bounded region near the unstable upside-down equilibrium.

The paper is outlined as follows. In Sec. 2, we describe the system of interest. Then the system dynamics in the absence of time delay is investigated. In the following Sec. 3, we present the first of the two main results of the paper. We analyse the system in the case of introducing small time delay. We show the existence and stability of symmetric small scale stable limit cycle of period 8τ. In fact, the birth of the limit cycles may be viewed as a type of Hopf-like bifurcation occurring due to the introduction of time delay into the system. These limit cycles undergo a symmetry breaking bifurcation. The following Sec. 4 is devoted to investigations of the system dynamics when the assumptions underlying the investigations of the system for small delay time no longer hold. In particular, we show the presence of a so-called event-collision bifurcation, period doubling route to chaos and an event-collision scenario of a homoclinic type. The second main result of the paper concerns the computation of the stability of asymmetric limit cycles following the event-collision bifurcations and presented

in Sec. 4.5. From the application point of view, what is especially intriguing is the fact that an onset of complex dynamics which we observe in the model system occurs for time delay equal to around $0.15ms$, and a characteristic delay time of signal conduction measured in neuromotorcontrol systems of humans is in the range 150ms [2, 3]. Sec. 5 concludes the paper and the directions for future investigations are highlighted.

2 System description

We consider the dynamics of a hybrid model system given by

$$\begin{aligned} \dot{\theta}(t) &= x(t), \\ \dot{x}(t) &= A\theta(t) + I(t), \end{aligned} \tag{1}$$

where

$$I(t) = \begin{cases} 0 \quad \text{for} \quad \theta(t-\tau)\dot{\theta}(t-\tau) < 0, \\ -K \quad \text{for} \quad \theta(t-\tau) \geq 0 \text{ and } \dot{\theta}(t-\tau) \geq 0, \\ K \quad \text{for} \quad \theta(t-\tau) \leq 0 \text{ and } \dot{\theta}(t-\tau) \leq 0, \end{cases} \tag{2}$$

and where A, K are some positive constants.

We are interested in investigating the dynamics in our intermittent controller with negative feedback control. In all numerical computations, we consider physiologically feasible values of the parameters with $A = 8.5347$, which corresponds to $h = 0.87m$. Of special interest, will be the range in the variations of the neural processing delay time τ of around 150ms, which is a typical delay time of the neuromuscular system [2, 3]. For our investigations we assume that K is set to 60% of the maximum torque generated by a falling body about the ankle joint axis (with $h = 0.87$) due to the gravitational acceleration acting on the body. In all numerical simulations presented we set $K = 5$.

2.1 System evolution as a concatenation of flows

Let the flow solution of the uncontrolled system (for I = 0) be denoted by ϕ_0, the flow solutions of the controlled system, with the control input $I = \mp K$, be denoted by ϕ_- and ϕ_+ respectively. We may describe limit cycle solutions using the composition of the system flows. Let $\phi_{kn} \circ \ldots \circ \phi_{k2} \circ \phi_{k1}$ denote a symmetric limit cycle solution obtained by composing a finite even number of flow segments, say $2n$ ($n \geq 2$), generated by ϕ_{ki}, where $k = 0$, $-$, or $+$, with integer i denoting the segment number. The system is invariant under the transformation $(\theta, x) \mapsto (-\theta, -x)$. This implies that if there exists an asymmetric limit cycle in the system, it has a symmetric counterpart with every point (θ, x) on the limit cycle replaced with $-(\theta, x)$, and with an appropriate replacement of flow segments ϕ_+ to ϕ_- or *vice versa*.

2.2 No delay in the system $\tau = 0$

2.2.1 Phase space topology

System (1) is easy to analyse for $\tau = 0$. First of all, in this case parameter K maybe scaled out and thus set to a unit value by introducing new variables $\bar{\theta} =$

θ/K and $\Delta = Kt$. We should note that in this case, proposed control, effectively, corresponds to changing the sign of the torque so that, should the stabilisation be effective, the system is bound to be stabilised within some neighbourhood of the origin. We will prove this below. For $\tau = 0$, switched system (1) is a Filippov type system with two perpendicular switching lines $\Sigma_1 = \{\theta = 0\}$ and $\Sigma_2 = \{\dot{\theta} = 0\}$. The state vector is (θ, x), where $x = \dot{\theta}$. We thus have vector fields

$$F_- = \begin{cases} x(t) \\ \mu\theta(t) - 1, \end{cases} \qquad F_+ = \begin{cases} x(t) \\ \mu\theta(t) + 1, \end{cases} \qquad F_0 = \begin{cases} x(t) \\ \mu\theta(t), \end{cases}$$

where after rescaling t and θ, we set $\mu = A/K > 0$. For the sake of convenience, we do not change variables θ and t to $\bar{\theta}$ and Δ, respectively. Vector field F_- governs the dynamics in the region of phase space where $\theta \geq 0$ and $\dot{\theta} \geq 0$, F_+ where $\theta \leq 0$ and $\dot{\theta} \leq 0$, and F_0 where $\theta\dot{\theta} < 0$. Clearly, on the switching lines we have two vector fields which influence the dynamics, and thus we obtain a system with a possibility of additional evolution on Σ_i $(i = 1, 2)$. Define $H_1(\theta, x) = \theta$ and $H_2(\theta, x) = x$, and let $L_{F_i}H_j$ denote the directional derivative of function H_j in vector field F_i, where $i =$ "+","-", or "0" and $j = 1, 2$. If on Σ_j the product of directional derivatives $(L_{F_\pm}H_j)(L_{F_0}H_j) > 0$ then on the switching lines the trajectories switch between the incoming and outgoing flow generated by the corresponding vector fields. By the incoming flow we mean the flow which in forward time reaches the switching surface and the outgoing flow is the flow which in forward time leaves the switching surface. On the other hand, if $(L_{F_\pm}H_j)(L_{F_0}H_j) < 0$ then there exists so-called sliding region on Σ_j. In this case, the vector fields on either side of the switching surface point towards it (or away from it) and so there exists the possibility of evolution on the switching surface, so-called *sliding evolution*. Let us first consider switching surface Σ_1. Clearly, on Σ_1 directional derivative $L_{F_\pm}H_1 = L_{F_0}H_1 = \theta$, and so $(L_{F_\pm}H_1)(L_{F_0}H_1) > 0$, which means that the system trajectories which reach Σ_1 cross the switching surface from vector field F_0 to F_- for positive θ, or from F_0 to F_+ for negative θ. Let us now consider switching surface Σ_2. On Σ_2, directional derivative $L_{F_\pm}H_1 = \mu\theta \pm 1$ and $L_{F_0}H_1 = \mu\theta$. Thus for $\theta \in (0, 1/\mu)$ or $\theta \in (-1/\mu, 0)$, there exists so-called *sliding region* on Σ_2, and for $\theta \in (1/\mu, \infty)$ or $\theta \in (-\infty, -1/\mu)$ the system trajectories which reach Σ_2 cross the switching surface. By means of Filippov convex method [8], we may now define a vector field which governs the dynamics on Σ_2 within the sliding region. That is, we have

$$F_s^{-0} = F_- + \alpha(F_0 - F_-), \quad \text{for} \quad \theta > 0, \tag{3}$$

or

$$F_s^{+0} = F_+ + \beta(F_0 - F_+), \quad \text{for} \quad \theta < 0, \tag{4}$$

where $0 \leq \alpha, \beta \leq 1$. We may use function $\alpha(\beta)$, together with the conditions on the directional derivative with respect to Σ_2 to determine the behaviour on Σ_2. For the sliding vector fields to lie on Σ_2, we require $L_{F_s^{-0}} = 0$ and $L_{F_s^{+0}} = 0$ on Σ_2, which gives

$$0 \leq \alpha = \frac{L_{F_-}H_2}{L_{F_- - F_0}H_2} \leq 1 \quad \text{and} \quad 0 \leq \beta = \frac{L_{F_+}H_2}{L_{F_+ - F_0}H_2} \leq 1.$$

We then obtain

$$0 \leq \alpha = -(\mu\theta - 1) \leq 1 \quad \text{and} \quad 0 \leq \beta = \mu\theta + 1 \leq 1.$$

Both these inequalities are satisfied. The first one for $\theta \in (0, 1/\mu)$ and the latter for $\theta \in (0, -1/\mu)$. Since $L_{F_- - F_0} H_2 = -1 < 0$, it implies $L_{F_-} H < 0$ for $\theta \in (0, 1/\mu)$, and the existence of so-called attracting sliding on Σ_2. Equivalently, since $L_{F_+ - F_0} H_2 = 1 > 0$, it implies $L_{F_+} H_2 > 0$ for $\theta \in (-1/\mu, 0)$ and, again, the existence of attracting sliding on Σ_2. Substituting the values of α, β into the equations for sliding vector fields, we obtain

$$F_s^{-0} = F_s^{+0} = \begin{cases} x \\ 0, \end{cases}$$

which is a zero vector since, by definition, on Σ_2 we have $x = 0$. Based on the above description of the phase space, we may now determine the asymptotic dynamics of the system, which is mostly determined by the position of the equilibria of vector fields $F_\pm$. It is easy to verify that these equilibria are equal to $x^*_{F_\pm} = \mp A^{-1} B = \mp(1/\mu, 0)^T$, where subscripts "$F_\pm$" correspond to vector fields F_+ and F_- respectively. Obviously, both equilibria have the same eigenvalues and eigenvectors, with the eigenvalues equal to $\lambda_{p/m} = \pm\sqrt{\mu}$, and the corresponding eigenvectors $\bar{x}_\pm = (1, \pm\sqrt{\mu})^T$. These equilibria are all of a saddle type, and as they lie on the switching line Σ_2 we will term them as pseudo-saddles. Moreover, pseudo-saddle F^*_- has the eigenvectors in the part of the phase space where $\theta > 0$ and $\dot{\theta} > 0$. Equivalently pseudo-saddle F^*_+ has the eigenvectors in the part of the phase space where $\theta < 0$ and $\dot{\theta} < 0$. We should note that there is also a pseudo-saddle at the origin, and it corresponds to vector field F_0. This pseudo-saddle has the same stable eigenvector, corresponding to the eigenvalue $\lambda_m = -\sqrt{\mu}$, as pseudo-saddles $x^*_{F_\pm}$.

2.2.2 Asymptotic dynamics

The trajectories rooted at points in the phase space where $\dot{\theta} > 0$, $\theta > 0$ and $\dot{\theta} \leq -\mu\theta + 1/\mu$ will evolve in finite time towards Σ_2 and remain on Σ_2 after reaching it. In other words, the subset of Σ_2 between $1/\mu > \theta > 0$ is a set of pseudo-equilibria (neutrally stable). For the initial points in this quadrant, but for which the condition $\dot{\theta} \leq -\mu\theta + 1/\mu$ is violated, the trajectories will converge towards the unstable manifold of the pseudo-saddle of F_- and so will diverge.

Similarly, the trajectories rooted at points in the phase space where $\dot{\theta} < 0$, $\theta < 0$ and $\dot{\theta} \geq \mu\theta - 1/\mu$ will evolve in finite time towards Σ_2 and remain on Σ_2 after reaching it. In other words, the subset of Σ_2 between $-1/\mu < \theta < 0$ is a set of pseudo-equilibria (neutrally stable). Similarly as in the previous case, for the initial points in this quadrant, but for which the condition $\dot{\theta} \geq -\mu\theta - 1/\mu$ is violated, the trajectories will converge towards the unstable manifold of the pseudo-saddle of F_+ and so will diverge.

Let us now consider the part of the phase space where $\theta < 0$ and $\dot{\theta} > 0$. There are two critical sets here which separate the trajectories which remain bounded and these which remain unbounded. These sets are given as the images of points $(-1/\mu, 0)$ and $(0, 1/\mu)$ under flow ϕ_0 for any $t < 0$. The latter is the point of intersection of the stable manifold of the pseudo-saddle of F_- with the $\dot{\theta}$ axis.

We will denote the first set by $\mathcal{L}^{(2)}$ and the latter by $\mathcal{U}^{(2)}$. All trajectories rooted at points from this quadrant, and bounded below (with respect to $|\dot{\theta}|$) by $\mathcal{L}^{(2)}$ and above by $\mathcal{U}^{(2)}$, will converge in finite time onto pseudo-equilibria of Σ_2. On the other hand, all trajectories rooted below $\mathcal{L}^{(2)}$ or above $\mathcal{U}^{(2)}$ will converge towards the unstable manifolds of the pseudo-saddles of $F_{\pm}$ respectively.

Equivalently, let us now consider the part of the phase space where $\theta > 0$ and $\dot{\theta} < 0$. There are two critical sets here which separate the trajectories which remain bounded and these which remain unbounded. These sets are given as the images of points $(1/\mu, 0)$ and $(0, -1/\mu)$ under the flow ϕ_0 for any $t < 0$. The latter point is the point of intersection of the stable manifold of the pseudo-saddle of F_+ with the $\dot{\theta}$ axis. We will denote the first bounding set by $\mathcal{L}^{(4)}$ and the latter by $\mathcal{U}^{(4)}$. All trajectories rooted at points from this quadrant, and bounded below by $\mathcal{L}^{(4)}$ and above by $\mathcal{U}^{(4)}$ (with respect to $|\dot{\theta}|$), will converge in finite time onto pseudo-equilibria of Σ_2. On the other hand, all trajectories rooted below $\mathcal{L}^{(4)}$ or above $\mathcal{U}^{(4)}$ will converge towards the unstable manifold of the pseudo-saddle of $F_{\pm}$ respectively.

We may finally determine what is the dynamics on switching manifolds Σ_1 and Σ_2. Consider first switching manifold Σ_2. Call the set of points on Σ_2 for $\theta \in (-1/\mu\,, 1/\mu)$ as $\hat{\Sigma}$. All points in $\hat{\Sigma}$ are neutrally stable pseudo-nodes. That is, any trajectory rooted on $\hat{\Sigma}$ will remain on a given point in $\hat{\Sigma}$. Also, any trajectory which reaches Σ_2 within this set, will remain in the set on a point which it reaches. Points $x^*_{F_{\pm}} = \mp(1/\mu, 0)$ are the aforementioned pseudo-saddles. All points on Σ_2 outside of $\hat{\Sigma}_2 \cup \{\theta_{\pm} = \pm 1/\mu\}$ are crossing points. That is, trajectories rooted on, or reaching, crossing points switch between vector fields F_- to F_0, or F_+ to F_0, on this part of switching set Σ_2.

Consider now switching manifold Σ_1. All points on Σ_1 except for the origin and the two intersection points of the stable eigenvectors of $x^*_{F_{\pm}}$ with Σ_1 are crossing points. That is, the trajectories rooted or reaching crossing points of Σ_1 switch from F_0 to F_- or from F_0 to F_+ on Σ_1.

3 The effect of small delay

We will now consider the dynamics of delayed system (1) and (2) under the introduction of small delay of $\mathcal{O}(\varepsilon)$ in the switching. However, we will consider the original vector fields (without rescaling). That is, we have

$$F_-^{\tau} = \begin{cases} x(t) \\ A\theta(t) - K, \end{cases} \quad \text{for} \quad \theta(t-\tau) \geq 0 \quad \text{and} \quad \dot{\theta}(t-\tau) \geq 0,$$

$$F_+^{\tau} = \begin{cases} x(t) \\ A\theta(t) + K, \end{cases} \quad \text{for} \quad \theta(t-\tau) \leq 0 \quad \text{and} \quad \dot{\theta}(t-\tau) \leq 0,$$

and

$$F_0^{\tau} = \begin{cases} x(t), \\ A\theta(t), \end{cases} \quad \text{for} \quad \theta(t-\tau)\dot{\theta}(t-\tau) < 0.$$

The reason for preserving the original parameters is that, due to the introduction of switching delay τ, the parameters affect the dynamics on different time scales and may be thought of as being independent, and hence we cannot reduce their number by rescaling.

We will now introduce so-called delay switching lines, which are sets in $(\theta, \dot{\theta})$ phase space where the actual switchings between the vector fields of the system take place for $\tau > 0$. As it was shown in [18], the system evolution may be defined by considering an initial segment of the trajectory which has a finite number of intersection points with the switching manifolds. The forward evolution is then determined by considering a $T-$ time image of these intersection points. Hence, even though the delay system is infinite dimensional, the dynamics itself is finite dimensional. The necessary condition for such a reduction is that the system trajectory intersects the switching manifold a finite number of times in the interval $[t-\tau,\, t]$, where $t \geq 0$ is some time instance, and $\tau > 0$ is a fixed delay time. Let us now suppose that we want to determine the dynamics of system trajectories which, within any time interval $[t-\tau,\, t]$, cross the switching manifolds only ones. We may determine the dynamics by considering the aforementioned delay switching lines, which are τ-time images of switching lines Σ_1 and Σ_2 under flows ϕ_i, where $i = 0, \pm$.

3.1 Delay switching points

Consider an arbitrary, but fixed delay time $\tau > 0$. Let $P_0 = (0,\, \dot{\theta}_0)$ be some point on Σ_1. Let us assume that there is no other crossing of Σ_i $(i = 1,\, 2)$ by a system trajectory rooted at P_0 during the time interval $[-\tau,\, \tau\,]$. Using pairs $(\theta(\tau), \dot{\theta}(\tau))$, which are τ images of any initial point P_0 under flow ϕ_0, the actual switching points between the vector fields are given by

$$\theta(\tau) = \frac{\dot{\theta}_0}{\sqrt{A}} \sinh(\sqrt{A}\tau), \;\; \dot{\theta}(\tau) = \dot{\theta}_0 \cosh(\sqrt{A}\tau),$$

where $\dot{\theta}_0 \in \mathbb{R}$. Assuming $\tau = \mathcal{O}(\varepsilon)$, to leading order in τ, we may approximate these switching points by

$$\theta(\tau) = \dot{\theta}_0 \tau, \;\; \dot{\theta}(\tau) = \dot{\theta}_0,$$

and so the set

$$\Sigma^{\varepsilon}_{\phi_0} = \{(\theta,\, \dot{\theta}) \in \mathbb{R}^2 \,:\, \tau\dot{\theta} = \theta\},$$

lies in some sufficiently small neigbourhood of the points where the actual switchings between vector fields F^{τ}_0 and $F^{\tau}_{\pm}$ take place (for sufficiently small delay times).

Similarly, let $P_1 = (0,\, \dot{\theta}_0)$ be some point on Σ_2. Let us assume that there is no other crossing of Σ_i $(i = 1,\, 2)$ by a system trajectory rooted at P_1 during the time interval $[-\tau,\, \tau\,]$. Using pairs $(\theta(\tau), \dot{\theta}(\tau))$, which are τ images of any initial point P_1 under flow $\phi_{\pm}$, the actual switching points between the vector fields are given by

$$\theta(\tau) = \theta_0 \cosh(\sqrt{A}\tau), \;\; \dot{\theta}(\tau) = \frac{A\theta_0 \pm K}{\sqrt{A}} \sinh(\sqrt{A}\tau).$$

Assuming $\tau = \mathcal{O}(\varepsilon)$, to leading order in τ, we may approximate the switching points as

$$\theta(\tau) = \theta_0, \;\; \dot{\theta}(\tau) = \frac{A\theta_0 \pm K}{\sqrt{A}} \sqrt{A}\tau,$$

and so the set

$$\Sigma^{\varepsilon}_{\phi_\pm} = \{(\theta,\, \dot{\theta}) \in \mathbb{R}^2 \,:\, A\theta\tau \pm K\tau = \dot{\theta}\},$$

approximates the set of points where the actual switchings between vector fields $F^{\tau}_{\pm}$ and F^{τ}_{0} take place (for sufficiently small delay times).

3.2 Small scale limit cycles. Numerical results

As it was shown in [18], the introduction of a delay in the switching function destroys the possibilities of sliding and hence the neutrally stable pseudo-equilibria which lie on Σ_2. From the expressions which give $\Sigma^{\varepsilon}_{\phi_i}$ (for $i = 0, \pm$), it follows that, if there exist symmetric, small scale limit cycles, value $|\dot{\theta}|$ on these limit cycles, at the points of switching, grows linearly in τ since $|\dot{\theta}| = K\tau$ to leading order in τ, and so it is of $\mathcal{O}(\varepsilon)$ for τ sufficiently small. Value $|\theta|$ on these limit cycles, at the points of switching, grows quadratically in τ since $|\theta| = K\tau^2$, and so it is of $\mathcal{O}(\varepsilon^2)$ for τ sufficiently small. This is schematically depicted in Fig. 1. In Fig. 1(a), we depict the values of the θ component of a periodic point on the limit cycle attractor at the point of switching (in the part of the phase space where $\theta > 0$, $\dot{\theta} > 0$) as a function of delay time τ. We note that the numerical values approach asymptotically the theoretical value of $K\tau^2$. The other parameters are set to $A = 8.5347$ and $K = 5$. In Fig. 1(b) the $\dot{\theta}$ component is depicted. Again, the expected asymptotic convergence of the $\dot{\theta}$ component at the point of switching, to the analytical value of $K\tau$, is clearly discernible.

3.3 Existence and stability of small scale limit cycles

The existence of delayed switching lines may be used to prove the existence and stability of small scale symmetric limit cycles, which are born due to the introduction of the switching delay. That is, we may derive a return map from Σ_1 (or Σ_2) back to itself, for some set of points for which the switchings take place on the delay switching lines described in the former section.

Consider switching line Σ_1 and some point $(0,\, \dot{\theta}_0) \in \Sigma_1$ with the history segment $\phi_0((0,\, \dot{\theta}), t)$, where $t \in [-\tau,\, 0]$ and with no intersection points of the history segment with Σ_i $(i = 1,\, 2)$. It follows that the switch to flow ϕ_- will take place after the delay time τ. There is a similar situation for an initial point on Σ_2. That is, for some point $(\theta_0,\, 0) \in \Sigma_2$ with the history segment $\phi_-((\theta_0,\, 0), t)$, where $t \in [-\tau,\, 0]$ and with no intersection points of the history segment with Σ_i $(i = 1,\, 2)$, the subsequent switch to flow ϕ_0 will take place after time τ.

Denote by ϕ^{τ}_i $(i = 0,\, -)$ a τ image of some point under the action of flow ϕ_i and by P so-called projection mappings, which are mappings that map points in some sufficiently small neighbourhood of the switching lines onto the switching lines following the flow. It then follows that if there exists a fixed point of the return map

$$\pi : (0,\, \dot{\theta}_0) \mapsto -P_{\phi_0}(\phi^{\tau}_0(\phi^{\tau}_-(P_{\phi_-}(\phi^{\tau}_-(\phi^{\tau}_0(0, \dot{\theta}_0))))))$$

for some point $(0,\, \dot{\theta}_0) \in \Sigma_1$, then there exists a small scale symmetric limit cycle in the system, and the period of the limit cycle is 8τ.

Let us denote points P_0 to P_6 as follows: (a) point $P_0 = (0,\, \dot{\theta}_0)$ is an initial point; (b) point $P_1 = (\theta_1,\, \dot{\theta}_1)$ is a point of switching between flow ϕ_0 and ϕ_-

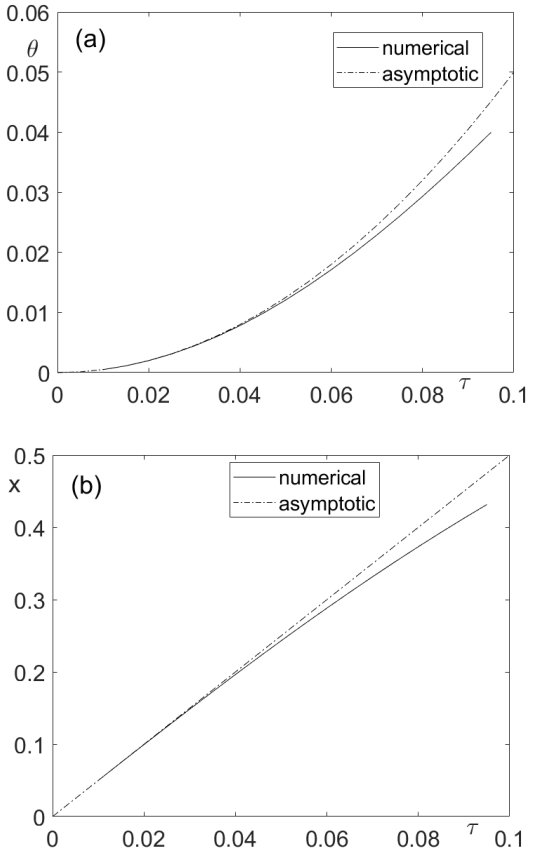

Figure 1: Scaling of the of small scale limit cycle attractors versus delay time τ at the switching points on the delay switching lines for $\theta > 0$ and $\dot{\theta} > 0$, and with the parameters set to $A = 8.5347$, $K = 5$. (a) Scaling of the θ component, and (b) scaling of the $\dot{\theta}$ component.

on the delay switching line after there elapses time τ; (c) point $P_2 = (\theta_2,\, \dot{\theta}_2)$ is a τ image of P_1, which lies in the neighbourhood of Σ_2; (d) point $P_3 \in \Sigma_2$ is an image of P_2 along the trajectory of flow ϕ_-; (e) point P_4 is a τ image of P_3 under the action of ϕ_- and so it again lies on the delay switching line; point P_5 is a τ image of P_4 and it lies in some neighbourhood of Σ_1; (f) finally $P_6 \in \Sigma_1$ is an image of P_5 along the trajectory of flow ϕ_-.

We will now obtain an explicit expression for π to determine the existence and stability of small scale limit cycles. We will do so by expanding the flows in τ. We thus have:

$$P_1 \;=\; \phi_0^\tau(0,\; \dot{\theta}_0) = \begin{cases} \dot{\theta}_0\tau + \frac{A}{6}\dot{\theta}_0\tau^3 + \mathcal{O}(\varepsilon^6), \\ \dot{\theta}_0 + \frac{A}{2}\dot{\theta}_0\tau^2 + \mathcal{O}(\varepsilon^5), \end{cases}$$

where $\mathcal{O}(\varepsilon^5)$ denote terms of the fifth order and higher (we interpret similarly $\mathcal{O}(\varepsilon^6)$). Thus to leading order in ε, $P_1 = (\dot{\theta}_0\tau,\, \dot{\theta}_0)$ where $\dot{\theta}_0\tau = \mathcal{O}(\varepsilon^2)$ and $\dot{\theta}_0 = \mathcal{O}(\varepsilon)$. In what follows we will express the subsequent points so that the θ component is expressed up to and including combined terms of $\mathcal{O}(\varepsilon^2)$ and the $\dot{\theta}$ component will include terms of $\mathcal{O}(\varepsilon^3)$. We then have

$$P_2 \;=\; \phi_-^\tau(P_1) = \begin{cases} 2\dot{\theta}_0\tau - \frac{K\tau^2}{2} + \mathcal{O}(\varepsilon^4), \\ \dot{\theta}_0 + \dot{\theta}_0\tau^2 + A\dot{\theta}_0\tau^2 - K\tau - \frac{1}{6}AK\tau^3 + \mathcal{O}(\varepsilon^5), \end{cases}$$

$$P_3 \;=\; P_{\phi_-}(P_2) = \begin{cases} 2\dot{\theta}_0\tau - \frac{K\tau^2}{2} + \mathcal{O}(\varepsilon^4), \\ 0, \end{cases}$$

$$P_4 \;=\; \phi_-^\tau(P_3) = \begin{cases} 2\dot{\theta}_0\tau - K\tau^2 + \mathcal{O}(\varepsilon^4), \\ 2A\dot{\theta}_0\tau^2 - K\tau - \frac{2}{3}AK\tau^3 + \mathcal{O}(\varepsilon^5), \end{cases}$$

$$P_5 \;=\; \phi_0^\tau(P_4) = \begin{cases} 2\dot{\theta}_0\tau - 2K\tau^2 + \mathcal{O}(\varepsilon^4) = 2\tau(\dot{\theta}_0 - K\tau) + \mathcal{O}(\varepsilon^4), \\ 4A\dot{\theta}_0\tau^2 - K\tau - \frac{13}{6}AK\tau^3 + \mathcal{O}(\varepsilon^5), \end{cases}$$

$$P_6 \;=\; P_{\phi_0}(P_5) = \begin{cases} 0, \\ 4A\dot{\theta}_0\tau^2 - K\tau - \frac{13}{6}AK\tau^3 + \mathcal{O}(\varepsilon^5). \end{cases}$$

We then have that the return map $\pi : \dot{\theta}_0 \mapsto \dot{\theta}_0$ is given by

$$\pi : \quad f(\dot{\theta}_0) = K\tau + \frac{13}{6}AK\tau^3 - 4A\dot{\theta}_0\tau^2 + \mathcal{O}(\varepsilon^5). \tag{5}$$

From the above functional expression for return map π, we may obtain the condition for the existence of a small scale periodic solution. We seek to obtain $\dot{\theta}_0$ as a power series in τ, where $\dot{\theta}_0 \in \Sigma_1$ is a periodic point on the limit cycle. Inverting the power series, we find that, to leading order in τ, $\dot{\theta}_0 = K\tau$. The stability of the limit cycle can be determined by computing the derivative $df/d\dot{\theta}_0$, which is $df/d\dot{\theta}_0 = -4A\tau^2$. Clearly, for τ sufficiently small $|df/d\dot{\theta}_0| = |4A\tau^2| < 1$ and hence the limit cycle is locally stable. Moreover, since the stability of the limit cycle is given by $|df/d\dot{\theta}_0|^2$ then, for sufficiently small τ, it may be regarded as being locally superstable since τ is close to 0.

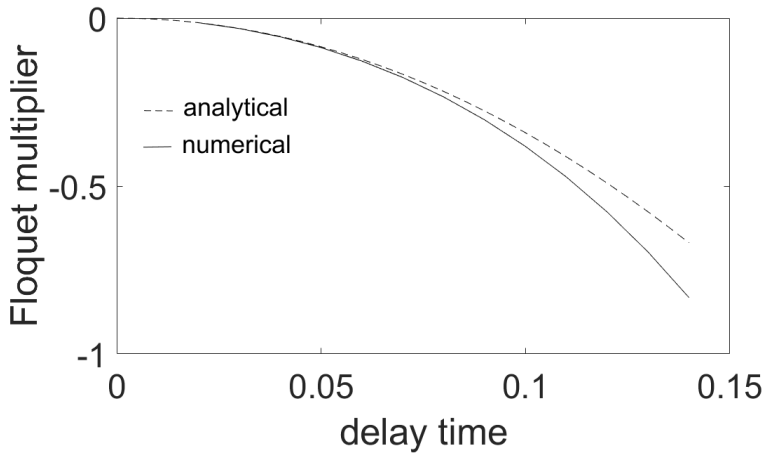

Figure 2: Scaling of the nontrivial Floquet multiplier corresponding to the small scale limit cycle attractor versus time delay. Asymptotic (dashed line) and numerical (solid line) results are shown.

3.4 Symmetry breaking bifurcation

In Fig. 2, we depict the value of the non-trivial Floquet multiplier of the limit cycle against delay time τ. Both, the numerical and analytical values, the latter computed from expression (5) for the Poincaré map, are shown. From presented numerical results, it can be seen that a symmetry breaking bifurcation is expected to take place for $\tau \approx 0.15$, where the multiplier takes the value equal to -1. From expression (5) by computing $df/d\theta_0$, we can approximate that the value of the delay time for which the Floquet multiplier is equal to -1 is equal to $\tau = 0.1711$. The above discrepancy is expected due to the fact that the Floquet multiplier approximated from expression (5) is based on asymptotic analysis for τ sufficiently small. We found that for $\tau = 0.15015$ the nontrivial Floquet multiplier is equal to -0.9963. Corresponding periodic orbit is shown in Fig.3(a). Thus the limit cycle, under further small variation of delay parameter τ will undergo a symmetry breaking bifurcation, and a pair of stable asymmetric limit cycles will be born in the bifurcation. Further variation of the bifurcation parameter leads to a fold bifurcation for $\tau \approx 0.15065$. An asymmetric stable limit cycle for $\tau = 0.15065$, that is "before" the fold bifurcation takes place, is depicted in Fig. 3(b). The nontrivial Floquet multiplier of the depicted limit cycle attractor has the value $\lambda = 0.9991$.

4 Arbitrary delay time

4.1 Event-collision leading to the birth of asymmetric limit cycle attractors

In this section, we numerically describe an event-collision bifurcation, which leads to the creation of a pair of asymmetric limit cycle attractors. This bifurcation, in the current case, is characterised by the fact that at the event-collision,

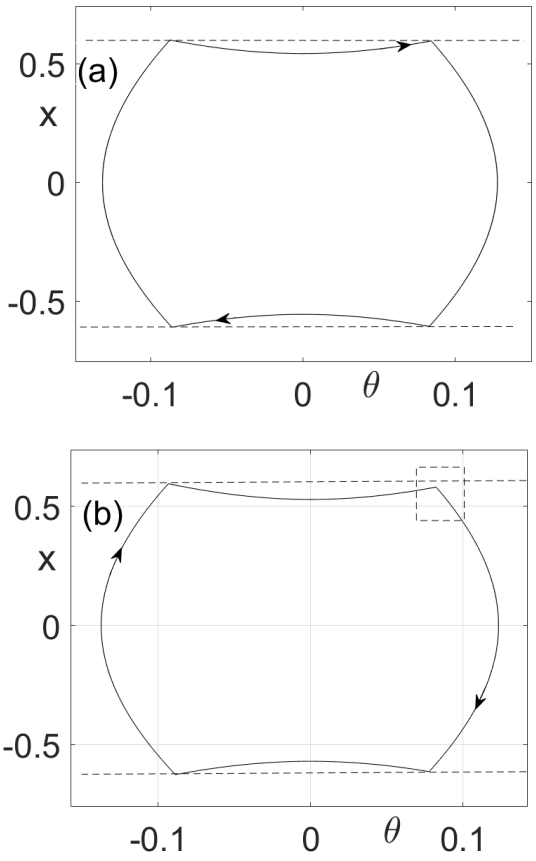

Figure 3: (a) An example of a symmetric limit cycle attractor for delay time set to $\tau = 0.15015$ and (b) and example of an asymmetric small scale limit cycle attractor after symmetry breaking bifurcation; delay time set to $\tau = 0.15065$. A dashed box and a dashed line are placed in the figure to highlight broken symmetry.

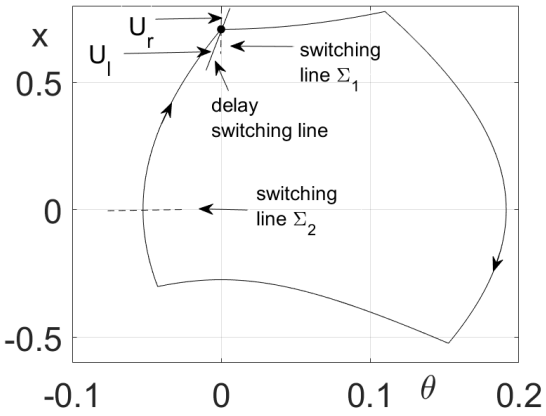

Figure 4: An asymmetric limit cycle attractor in intermittent control system (1) for $A = 8.5347$, $K = 5$ and $\tau = 0.15058$.

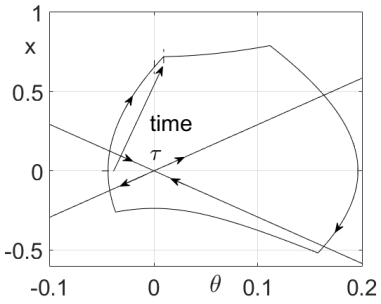

Figure 5: An asymmetric limit cycle attractor in intermittent control system (1) for $A = 8.5347$, $K = 5$ and $\tau = 0.1508$.

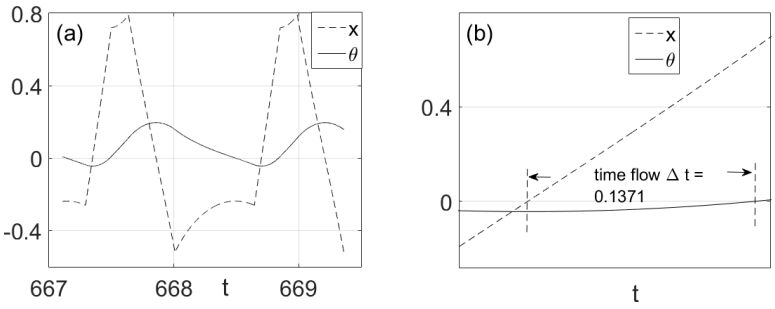

Figure 6: (a) Time series plots of the angular position and velocity components of an asymmetric limit cycle attractor in intermittent control system (1) for $A = 8.5347$, $K = 5$ and $\tau = 0.1508$ and (b) zoom depicting the segments between crossing of the θ and $\dot{\theta}$ axes by the system's flow.

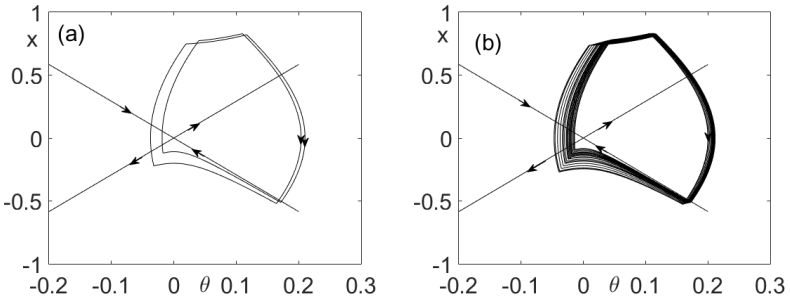

Figure 7: (a) Period-two limit cycle attractor in intermittent control system (1) for $A = 8.5347$, $K = 5$ and $\tau = 0.1545$, and (b) a chaotic attractor for $\tau = 0.1549$.

the bifurcating limit cycle is built of a trajectory segment which has the duration of delay time τ, and this segment joins the switching lines $\{\dot{\theta}(t) = 0\}$ and $\{\theta(t) = 0\}$. Such a limit cycle is born at $\tau^* = 0.15058$ (see Fig. 4). In fact, we observed an event-collision bifurcation of a saddle-node type. In Fig. 5, we depict an asymmetric limit cycle attractor for $\tau = 0.1508$. In the figure, we can discern a short segment of trajectory, generated by flow ϕ_+, existing past set $\{\theta(t) = 0\}$. In Fig. 6(a), we depict time series plots of θ and $x = \dot{\theta}$ states. In the zoom depicted in Fig. 6(b), we can see that the time taken by the flow to reach the $\dot{\theta}$ axis from the θ axis is approximately equal to $\Delta t = 0.1371$, which is close to delay time $\tau = 0.1508$.

4.2 Period-doubling bifurcation

Increasing bifurcation parameter τ leads to a period-doubling bifurcation of the two asymmetric limit cycle attractors. We observe a period-doubling cascade which leads to the onset of chaos. A period-two attractor is depicted in Fig. 7(a) for $\tau = 0.1545$. Increasing τ to $\tau = 0.1549$ leads to chaotic dynamics, which is depicted in Fig. 7(b). We should note here that the birth of chaos as described here is triggered by a "classical" period-doubling route to chaos, and hence we

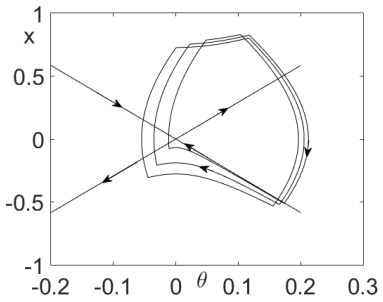

Figure 8: A period-three limit cycle attractor for $\tau = 0.1551$ implying the existence of chaos.

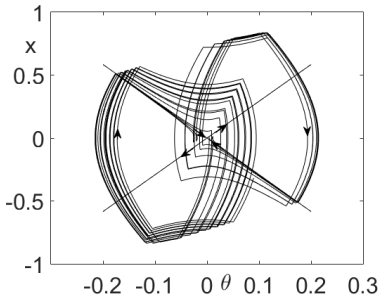

Figure 9: A chaotic attractor for $\tau = 0.156$.

expect periodic windows. Indeed a period-three attractor has been observed for $\tau = 0.1551$, see Fig. 8.

4.3 Homoclinic event-collision bifurcation

The chaotic attractor undergoes a homoclinic event-collision bifurcation. In this scenario, the time required by flow ϕ_- to move from a point of crossing set $\{\dot{\theta} = 0\}$ to reach the stable manifold of the saddle point is exactly equal to delay time τ. This bifurcation leads to merging of the two asymmetric chaotic attractors. An example of a chaotic attractor existing for $\tau = 0.156$ is depicted in Fig. 9.

4.4 Multistability

From the results presented in Sec. 3.4 and Sec. 4.1, it follows that there is a range of parameter values where we observe a co-existence of attractors. Namely, "after" the event collision at $\tau = 0.15058$ and "before" the fold bifurcation at $\tau = 0.15066$. An example of two stable limit cycles existing in this range of parameters is shown in Fig. 10 ($\tau = 0.15065$). The symmetric counterparts of these two limit cycles are also present in the system. We should note here that there are possible other ranges of parameter values where multistability is also present.

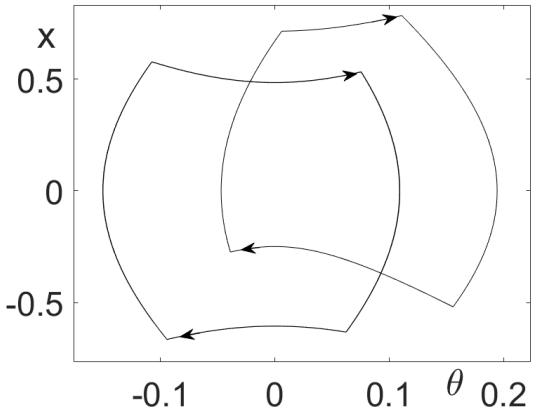

Figure 10: Co-existing two stable limit cycle attractors for $\tau = 0.15065$.

4.5 Analysis

Nonsmooth fold To describe the first event-collision bifurcation, we may use the composition of linear maps and the result of the normal form derivation of the event-collision bifurcation given in [18]. Consider now a sufficiently small neighbourhood, say $\mathcal{U}$, of periodic point $EC^* = (\theta^*, x^*) \in \Sigma_1$. To describe the system dynamics for all points (θ, x) from some sufficiently small neighbourhood, say $\mathcal{U}$ of (θ^*, x^*) we may derive a map $\mathcal{U} \mapsto \mathcal{U}$. In Fig. 4, we denote by U_l the set of points in $\mathcal{U}$ which in reverse time, under the action of flow ϕ_+, cross Σ_2, and the forward time-τ images of these points, which now lie on Σ_2, under the flow ϕ_+ do not lie to the right of Σ_1. Equivalently, in Fig. 4, we denote by U_r the set of points in $\mathcal{U}$ which in reverse time, under the action of flow ϕ_+, reach Σ_2, and the forward time-τ images of these points, which now lie on Σ_2, under the flow ϕ_+ lie to the right of Σ_1. A linear approximation of a map, say P, which maps $\mathcal{U} \mapsto \mathcal{U}$, can now be given as a composition of the solutions of the variational equations for the trajectory segments generated by flows ϕ_i $(i = \pm, 0)$ and the discontinuity mappings which take into account the presence of switching events. We also need to include in the map composition the discontinuity normal form map for the event-collision bifurcation. In our case, this leads the following linear approximation for P:

$$P((\theta,\, x)) = (\theta^*,\, x^*)^T + \begin{cases} \hat{A}(\theta - \theta^*,\, x - x^*)^T + \mathcal{O}(||\mathbf{x}||^2) & \text{for} \quad (\theta, x) \in U_r, \\ \bar{A}(\theta - \theta^*,\, x - x^*)^T + \mathcal{O}(||\mathbf{x}||^2) & \text{for} \quad (\theta, x) \in U_l, \end{cases}$$

where $\mathbf{x} = (\theta,\, x)^T$.
Matrices $\hat{A}$ and $\bar{A}$ have the following form

$$\begin{aligned} \hat{A} \;=\; & \partial\phi_+(x_3', \tau) \left[I - \frac{F_+^\tau h_x^d}{h_x^d F_+^\tau} \right] \partial\phi_+(x_3, t_3^*) \partial\phi_0(x_2', \tau) \\ & \left[I - \frac{F_0^\tau h_x^p}{h_x^p F_0^\tau} \right] \partial\phi_0(x_2, t_2^*) \partial\phi_-(x_1, \tau) \left[I - \frac{F_-^\tau h_x^d}{h_x^d F_-^\tau} \right] \partial\phi_-(x_1, t_1^*) \partial\phi_0(x^*, \tau) L M_1, \end{aligned}$$

and

$$\begin{aligned}\bar{A} &= \partial\phi_+(x_3',\tau)\left[I-\frac{F_+^\tau h_x^d}{h_x^d F_+^\tau}\right]\partial\phi_+(x_3,t_3^*)\partial\phi_0(x_2',\tau)\\ &\quad\left[I-\frac{F_0^\tau h_x^p}{h_x^p F_0^\tau}\right]\partial\phi_0(x_2,t_2^*)\partial\phi_-(x_1,\tau)\left[I-\frac{F_-^\tau h_x^d}{h_x^d F_-^\tau}\right]\partial\phi_-(x_1,t_1^*)\partial\phi_0(x^*,\tau)LM_2,\end{aligned}$$

where

$$LM_1 = I-\frac{F_0^\tau h_x^p}{h_x^p F_+^\tau} \quad \text{and} \quad LM_2 = I-\frac{F_0^\tau h_x^p}{h_x^p F_0^\tau}.$$

In expression above LM_1 and LM_2 are matrices representing the leading order term of the discontinuity normal form map for the event-collision bifurcation [18]. The matrices $\left[I-\frac{F_i^\tau h_x^k}{h_x^k F_i^\tau}\right]$ ($i=\pm,0,\ k=p,\ d$) are linear parts of the discontinuity mappings for transversal switchings of the flows solutions, and $\partial\phi(,)$ represents a solution of the variational equation of the flow solutions. Thus in our case, we have

$$\partial\phi_i(x,t) = \begin{pmatrix} \cosh(\sqrt{A}t) & \frac{1}{\sqrt{A}}\sinh(\sqrt{A}t) \\ \sqrt{A}\sinh(\sqrt{A}t) & \cosh(\sqrt{A}t) \end{pmatrix},$$

$i=\pm,0$. Finally, h_x^p and h_x^d may be represented as vectors normal to Σ_1 and Σ_2 respectively, and the relevant quantities in the expression above may be computed using the standard rules of matrix multiplication.

Since the system is piecewise-linear, we may find the event-collision bifurcation point using explicit flow solutions. Writing down a set of five equations for the unknown periodic point (θ^*, x^*) ($\theta^*=0$ on Σ_1) and times τ, t_1, t_2 and t_3 (see the Appendix for details), we found $x^*=0.70782$, $\tau=0.15058$, $t_1=0.21627$, $t_2=0.43255$ and $t_3=0.06569$. We found that at the event collision bifurcation the non-trivial Floquet multiplier corresponding to the limit cycle solution is equal to 1.00 and hence we observe an event collision bifurcation of the fold type. In our case LM_1 and LM_2 are the same due to the structure of the system, which, generically, is not the case at the event-collision bifurcation. Thus, generically, at an event-collision bifurcation a piecewise-linear map describes the dynamics.

Stability of limit cycles past the event-collision For the parameter values past the event-collision bifurcation (in our case it means for $\tau > 0.15058$), to determine the stability of the limit cycle attractor born in the nonsmooth fold bifurcation, we need a composition of linear maps for the different segments of the limit cycle attractor which make up the whole invariant orbit. Consider a neighbourhood of a periodic point $(\theta^*,\ x^*)$ on the limit cycle, with $\theta^*>0$ and $x^*>0$ where the flow switches between ϕ_0 and ϕ_-. The attractor, say LC, may then be described by a composition of the following flows

$$LC\ :\ \phi_0\circ\phi_+\circ\phi_0\circ\phi_-.$$

The linearisation about $(\theta^*,\ x^*)$ may be obtained by considering a composition of linear maps derived from the variational equations for the flows $\phi_\pm$ and ϕ_0,

combined together the discontinuity maps which take into account the effects of switchings. Let

$$\partial\phi_i(x,t)$$

denote the variational matrix for a specific flow segment $\phi_i(x,t)$ over some time t, for $i = 0, \pm$. Consider now a sufficiently small neighbourhood, say $\mathcal{U}$, of the point $(\theta^*,\, x^*)$. A linear approximation of a map, say P, which maps $\mathcal{U} \mapsto \mathcal{U}$, can be given by

$$P((\theta,\, x)) = (\theta^*,\, x^*)^T + A(\theta - \theta^*,\, x - x^*)^T + \mathcal{O}(||\mathbf{x}||^2),$$

where $\mathbf{x} = (\theta,\, x)^T$. We write $A = A_3A_2A_1$ to highlight a subtle difference in the flow composition and the effect of the event-collision bifurcation on the stability of the limit cycles away from the bifurcation point. We have

$$A_1 = \partial\phi_0(x_2', \tau)\left[I - \frac{F_0^\tau h_x^p}{h_x^p F_0^\tau}\right]\partial\phi_0(x_2, t_2^*)\partial\phi_-(x_1,\tau)\left[I - \frac{F_-^\tau h_x^d}{h_x^d F_-^\tau}\right]\partial\phi_-(x^*, t_1^*),$$

$$A_2 = \left[I - \frac{(F_+^\tau - F_0^\tau)h_x^{d\tau}}{h_x^{d\tau}F_+^\tau}\right]\partial\phi_+(x_4,t_4)\left[I - \frac{F_+^\tau h_x^p}{h_x^p F_+^\tau}\right]\partial\phi_+(x_3', \tau - t_4)\left[I - \frac{F_+^\tau h_x^d}{h_x^d F_+^\tau}\right]\partial\phi_+(x_3, t_3^*),$$

and

$$A_3 = \partial\phi_0(x_4', \tau - t_4).$$

Let us now look in closer detail at the expressions for matrices A_1, A_2 and A_3. Matrix A_1 takes into account the effects of the variation from the initial point $(\theta,\, x^*)$ until the switching point from flow ϕ_0 to ϕ_+ takes place (for $\theta < 0$ and $\dot{\theta} < 0$). This is a standard variational matrix containing the effects of switchings and it contains, correspondingly, the same terms as variational matrices $\bar{A}(\hat{A})$. If we now consider matrix A_2, the first two terms on the right have counterparts in $\bar{A}(\hat{A})$. However, the segment of the trajectory building-up a limit cycle from Σ_2 to the next switching, which will take place after time τ but, also, after crossing of Σ_1, has to be broken down into two parts. One part is the part from Σ_2 to Σ_1 with the duration of $\tau - t_4$ and the second part is the part from Σ_2 to the actual switching point, and so three variational matrices are obtained. And here comes a subtle effect of the event collision on the composed variational matrix. The leftmost term of A_2 contains term

$$\left[I - \frac{(F_+^\tau - F_0^\tau)h_x^{d\tau}}{h_x^{d\tau}F_+^\tau}\right]. \tag{6}$$

This term captures the effect which has the switching between flows, after crossing of Σ_1, on the variational matrix for points crossing Σ_1. We should note that the time from crossing Σ_1 to the next switching to flow ϕ_- must be exactly equal to τ, and hence the combined time of the evolution of flows ϕ_+ and ϕ_0 must be equal to τ, and so the discontinuity map which captures the effects of switching on the variational matrix must take zero time. This additional variation is computed with respect to the delayed switching line, which is a τ image of Σ_2 under the action of flow ϕ_+. Vector $h_x^{d\tau} = [1,\, -\sqrt{A}/\tanh(\sqrt{A}\tau)]$ is a vector normal to the delayed switching line.

Matrix A_3 is a standard variational matrix. However, from the presented matrix composition, it is clear that the effect of the event-collision on the limit

cycle may be significant even for a slight change of the delay time τ which, effectively, translates onto an additional variational matrix (6). Indeed, we observed this to be the case, and when we computed the variational matrices A_1, A_2 and A_3 for $\tau = 0.151$, we found that the non-trivial Floquet multiplier for the asymmetric limit cycle attractor born in the event-collision bifurcation is equal to -0.45052, which is a significant variation from the value of 1 for such a small range of parameter variation – from $\tau = 0.15058$ to $\tau = 0.151$. Further variation of τ leads to a standard period-doubling bifurcation and a period-doubling route to chaos, which may be verified by computing the values of the non-trivial Floquet multipliers for the limit cycles. The analysis presented in this section further clarifies the observed numerical results, and it explains why there is such a drastic change in the stability of the limit cycle attractors past the event-collision bifurcation.

5 Conclusions

In the paper, we consider a switched control system with a time delay in the switching function, which we considered to be a macroscopic model of human neuromotorcontrol system for diverse tasks such as, for example, target tracking or human balance control [2, 3, 12]. We first investigate the system dynamics in the absence of time delay. We find a set of neutrally stable pseudo-equilibria, which are $\Omega-$limit sets for all bounded trajectories of the system. The phase space is divided into parts where, in forward time, system trajectories tend to these pseudo-equilibria, and parts where the trajectories are unbounded. It is the stable and unstable manifolds of the pseudo-saddles which divide the phase space into different parts.

Then in Sec. 3, we investigate the effect of introducing small time delay in the switching function. By means of asymptotic analysis, we prove the existence and stability of small scale limit cycle attractors which are born when the delay time is switched on. The so-called delay switching lines are crucial for their existence. Their presence allows to reduce the analysis of the system dynamics to the analysis of finite dimensional maps. In particular, we show that the period of the small scale symmetric limit cycle attractors is dependent of the switching lines and constrained by the delay time, and for delay time τ the period is equal to 8τ. Then in Sec. 4, we show the presence of the so-called event-collision bifurcation scenario of the fold type, which is followed by a period-doubling route to chaos. The presence of multiple number of stable limit cycle attractors are also shown. Finally, a homoclinic event-collision bifurcation is also shown. By means of local analysis, we show the particular effect that the event-collision bifurcation has on the stability of a limit cycle attractor born in the bifurcation. In particular, we show that even small changes of the parameter (delay time) may significantly change the stability of the limit cycle attractor because an additional discontinuity mapping has to be included to account for an event-collision bifurcation for parameter values "after" ("before") the bifurcation.

The analytical and numerical findings of the paper seem to have important implications in the context of human neuromotorcontrol systems. We discover much complexity in the system - bifurcations, multistability and period-doubling route to chaos in the range of the delay time of around 150ms. At the same time, the typical delay time of neural processing in humans during different

tasks such as, for example, the control of posture during quiet standing is in the range of 150ms. We conjecture that pathologies of human neuromotorcontrol system are related to the loss of the observed dynamical complexity for this range of neural processing delay. The reason behind such a conjecture is that in biomechanics literature complexity measures such as sample entropy (from information theory) seem to signify that higher complexity of experimental data corresponding to some control tasks reflect healthy neuromuscular control system [7, 17]. Future experimental work related to the presented macroscopic model is directed towards experimental validation of proposed hypothesis. We will seek to find the evidence that such a structure can be discerned in neuromotorcontrol systems, especially in the context of the act-and-wait control. The theoretical work will further explore the importance of delay switching lines on system dynamics, and their effect on the stability of limit cycle attractors following event-collision bifurcations. In terms of relevance to applications, it is also interesting to investigate further the relationship between the period of small scale limit cycle attractors, the delay time and the stability. In our case, the period of small scale limit cycle attractors was equal to 8τ (with τ being the delay time), and for sufficiently small delay time the limit cycle is characterised by the value of the non-trivial Floquet multiplier close to zero.

Appendix

To detect numerically the limit cycle at the event-collision, we us the explicit flow solutions. Namely, we have

$$\phi_0 : \begin{cases} \theta(t) = \dfrac{\dot\theta_0}{\sqrt{A}} \sinh(\sqrt{A}t) + \theta_0 \cosh(\sqrt{A}t) \\ \dot\theta(t) = \dot\theta_0 \cosh(\sqrt{A}t) + \sqrt{A}\theta_0 \sinh(\sqrt{A}t), \end{cases}$$

$$\phi_+ : \begin{cases} \theta(t) = \dfrac{A\theta_0 + K}{A} \cosh(\sqrt{A}t) + \dfrac{\dot\theta_0}{\sqrt{A}} \sinh(\sqrt{A}t) - \dfrac{K}{A} \\ \dot\theta(t) = \dot\theta_0 \cosh(\sqrt{A}t) + \dfrac{A\theta_0 + K}{\sqrt{A}} \sinh(\sqrt{A}t), \end{cases}$$

and

$$\phi_- : \begin{cases} \theta(t) = \dfrac{A\theta_0 - K}{A} \cosh(\sqrt{A}t) + \dfrac{\dot\theta_0}{\sqrt{A}} \sinh(\sqrt{A}t) + \dfrac{K}{A} \\ \dot\theta(t) = \dot\theta_0 \cosh(\sqrt{A}t) + \dfrac{A\theta_0 - K}{\sqrt{A}} \sinh(\sqrt{A}t). \end{cases}$$

We consider the four trajectory segments which make up the limit cycle attractor, and denote initial points for each trajectory segment after the colon mark. Thus, we have

$$\phi_0 : \ (0, \dot\theta_1), \qquad \phi_- : \ (\theta_2, \dot\theta_2), \qquad \phi_0 : \ (\theta_3, \dot\theta_3) \quad \text{and} \quad \phi_+ : \ (\theta_4, \dot\theta_4).$$

Define

$$\begin{aligned}
\theta_2 &= \frac{\dot{\theta}_1}{\sqrt{A}}\sinh(\sqrt{A}\tau),\\
\dot{\theta}_2 &= \dot{\theta}_1\cosh(\sqrt{A}\tau),\\
\theta_3 &= \frac{A\theta_2 - K}{A}\cosh(\sqrt{A}(t_1+\tau)) + \frac{\dot{\theta}_2}{\sqrt{A}}\sinh(\sqrt{A}(t_1+\tau)) + \frac{K}{A},\\
\dot{\theta}_3 &= \dot{\theta}_2\cosh(\sqrt{A}(t_1+\tau)) + \frac{A\theta_2 - K}{\sqrt{A}}\sinh(\sqrt{A}(t_1+\tau)),\\
\theta_4 &= \frac{\dot{\theta}_3}{\sqrt{A}}\sinh(\sqrt{A}(t_2+\tau)) + \theta_3\cosh(\sqrt{A}(t_2+\tau)),\\
\dot{\theta}_4 &= \dot{\theta}_3\cosh(\sqrt{A}(t_2+\tau) + \sqrt{A}\theta_3\sinh(\sqrt{A}(t_2+\tau)).
\end{aligned}$$

We can now write a set of five equations for the five unknown quantities t_1, t_2, t_3, τ and $\dot{\theta}_1$. We get

$$0 = \frac{A\theta_4 + K}{A}\cosh(\sqrt{A}(t_3+\tau)) + \frac{\dot{\theta}_4}{\sqrt{A}}\sinh(\sqrt{A}(t_3+\tau)) - \frac{K}{A}, \quad (7)$$

$$\dot{\theta}_1 = \dot{\theta}_4\cosh(\sqrt{A}(t_3+\tau)) + \frac{A\theta_4 + K}{\sqrt{A}}\sinh(\sqrt{A}(t_3+\tau)), \quad (8)$$

$$0 = \dot{\theta}_2\cosh(\sqrt{A}t_1) + \frac{A\theta_2 - K}{\sqrt{A}}\sinh(\sqrt{A}t_1), \quad (9)$$

$$0 = \frac{\dot{\theta}_3}{\sqrt{A}}\sinh(\sqrt{A}t_2) + \theta_3\cosh(\sqrt{A}t_2), \quad (10)$$

$$0 = \dot{\theta}_4\cosh(\sqrt{A}t_3) + \frac{A\theta_4 + K}{\sqrt{A}}\sinh(\sqrt{A}t_3). \quad (11)$$

Acknowledgements
This research did not receive any specific grant from funding agencies in the public, commercial, or not-for-profit sectors.

References

[1] J Adolfsson, H Dankowicz, and A Nordmark. 3D passive walkers: Finding periodic gaits in the presence of discontinuities. *Nonlinear Dynamics*, 24:205–229, 2001.

[2] A Bottaro, M Casadio, P Morasso, and V Sanguineti. Body sway during quiet standing: Is it theresidual chattering of an intermittent stabilization process? *Human Movement Science*, 24:588–615, 2005.

[3] A Bottaro, Y Yasutake, T Nomura, M Casadio, and P Morasso. Bounded stability of the quiet standing posture:an intermittent control model. *Human Movement Science*, 27:473–495, 2008.

[4] S. Coombes, Y. M. Lai, M. Sayli, and R. Thul. Networks of piecewise linear neural mass models. *European Journal of Applied Mathematics*, 29(Special Issue 5 (Theory and applications of nonsmooth dynamical systems)):869–890, 2018.

[5] M. di Bernardo, C. J. Budd, A. R. Champneys, and P. Kowalczyk. *Piecewise-smooth Dynamical Systems: Theory and Applications*. Springer-Verlag, 2008.

[6] M. di Bernardo, A. Nordmark, and G. Olivar. Discontinuity-induced bifurcations of equlibria in piecewise-smooth and impacting dynamical systems. *Physica D*, 237:119–136, 2008.

[7] M. Duarte and D. Sternad. Complexity of human postural control in young and older adults during prolonged standing. *Experimental Brain Research*, 191:265–276, 2008.

[8] A. F. Filippov. *Differential Equations with Discontinuous Righthand Sides*. Kluwer Academic Publishers, Dortrecht, 1988.

[9] J. S. Hogan. On the dynamics of a rigid block, tethered at one corner, under harmonic forcing. *Proceedings of the Royal Society London A*, 439:35–45, 1992.

[10] Tamás Insperger, László L. Kovács, Péter Galambos, and Gábor Stépán. Act-and-wait control concept for a force control process with delayed feedback. In Heinz Ulbrich and Lucas Ginzinger, editors, *Motion and Vibration Control*, pages 133–142, Dordrecht, 2009. Springer Netherlands.

[11] P. Kowalczyk. A novel route to a hopf-bifurcation scenario in switched systems with dead zone. *Physica D*, 348:60–66, 2017.

[12] P. Kowalczyk, P. Glendinning, Martin Brown, Gustavo Medrano-Cerda, Houman Dallali, and Jonathan Shapiro. Modelling human balance using switched systems with linear feedback control. *Journal of the Royal Society Interface*, 9:234–245, 2011.

[13] Yu.A. Kuznetsov, S. Rinaldi, and A. Gragnani. One-parameter bifurcations in planar filippov systems. *Int. J. Bifurcation Chaos*, 13:2157–2188, 2003.

[14] R.I. Leine. *Bifurcations in Discontinuous Mechanical Systems of Filippov-Type*. PhD thesis, Teknische Universiteit Eindhoven, The Netherlands, 2000.

[15] I. Loram, H. Gollee, M. Lakie, and P. Gawthrop. Human control of an inverted pendulum: Is continuous control necessary? is intermittent control effective?is intermittent control physiological? *The Journal of Physiology*, 589(2):307–324, 2011.

[16] J. Milton, T. Insperger, and G. Stépán. Human Balance Control: Dead Zones, Intermittency, and Micro-Chaos.*, Mathematical Approaches to Biological Systems*. Springer, 2015.

[17] S. Nema, P. Kowalczyk, and I. Loram. Complexity and dynamics of switched human balance control during quiet standing. *Journal of Biological Cybernetics*, 109:469–478, 2015.

[18] J. Sieber. Dynamics of delayed relay systems. *Nonlinearity*, 19:2489–2527, 2006.

[19] J. Sieber, P. Kowalczyk, S. J. Hogan, and M. di Bernardo. Dynamics of symmetric dynamical systems with delayed switching. *Journal of Vibration and Control*, 16:1111–1140, 2010.

[20] D. J. W. Simpson, R. Kuske, and Y.-X. Li. Dynamics of simple balancing models with time-delayed switching feedback control. *Journal of Nonlinear Science*, 22(2):135–167, 2012.